Chapter 35
Coherent Diffraction Imaging with Tabletop XUV Sources

M. Zürch, A. Guggenmos, R. Jung, J. Rothhardt, C. Späth, J. Tümmler, S. Demmler, S. Hädrich, J. Limpert, A. Tünnermann, U. Kleineberg, H. Stiel and C. Spielmann

Abstract Coherent diffraction imaging (CDI) at wavelengths in the extreme ultraviolet range has become an important tool for nanoscale investigations. Employing laser-driven high harmonic sources allows for lab-scale applications such as cancer cell classification and phase-resolved surface studies in reflection geometry. The excellent beam properties support a spatial resolution below the wavelength, i.e., close to the Abbe limit. Unfortunately, the usually low photon flux of HHG sources limits their applicability. Recent advances in ultrafast fiber laser development cumulated in sources delivering average powers approaching the milliwatt level in the extreme ultraviolet. In comparison, a tabletop soft X-ray laser driven by moderate pump energies was recently employed for CDI featuring excellent temporal coherence and extraordinary high flux allowing for single-shot imaging.

M. Zürch (✉)
Chemistry Department, University of California, Berkeley, USA
e-mail: mwz@berkeley.edu

M. Zürch · C. Spielmann
Institute of Optics and Quantum Electronics, Jena University, Jena, Germany

M. Zürch · J. Rothhardt · S. Hädrich · J. Limpert · A. Tünnermann · C. Spielmann
Helmholtz Institute Jena, Jena, Germany

A. Guggenmos · C. Späth · U. Kleineberg
Ludwig-Maximilians-Universität München, Garching, Germany

A. Guggenmos · C. Späth · U. Kleineberg
Max-Planck-Institut für Quantenoptik, Garching, Germany

R. Jung · J. Tümmler · H. Stiel
Max Born Institute, Berlin, Germany

J. Rothhardt · S. Demmler · S. Hädrich · J. Limpert · A. Tünnermann
Institute of Applied Physics, Jena University, Jena, Germany

J. Limpert · A. Tünnermann
Fraunhofer Institute for Applied Optics and Precision Engineering, Jena, Germany

T. Kawachi et al. (eds.), *X-Ray Lasers 2016*, Springer Proceedings in Physics 202, https://doi.org/10.1007/978-3-319-73025-7_35

35.1 Introduction

The short wavelength radiation in the extreme ultraviolet (XUV) and soft X-ray range together with a high photon flux are the key elements for imaging nanoscopic structures. Coherent diffraction imaging (CDI) suits the needs for imaging in the XUV by omitting optical elements that would typically introduce high losses and limit the numerical aperture and thus the achievable resolution [1]. For the broader application of this technique, laboratory light sources of various kinds have been applied.

A prominent compact source increasingly applied for coherent diffraction imaging and holography at short wavelengths is based on high-order harmonic generation [2]. Such sources are driven by an amplified ultrafast laser system and feature high spatial coherence with sufficient narrowband emission lines. The latter is important for realizing temporal coherence that allows imaging down to the wavelength scale as has been recently demonstrated [3]. The spectral range covered with high photon flux by these sources is typically several 10 eV up to several 100 eV. Due to the low penetration depth at these photon energies, recent applications targeted the reflection geometry [4, 5] where CDI becomes a powerful technique yielding three-dimensional information of the surface. In addition, material specificity can be achieved [6]. The surface sensitivity becomes advantageous when nano- and microscale objects of a certain morphology are to be compared or classified. As an example, recently it was demonstrated that reflection geometry CDI at 35 eV photon energy can be used to classify different breast cancer cell expression profiles, solely by investigation of their diffraction patterns [7]. Other recent trends include using the full frequency comb of a harmonic source for gaining additional information comparable to Fourier transform spectroscopy [8] or raster scanning the sample, the so-called ptychography, for increasing the field of view and relaxing constraints in the image reconstruction [9].

In this contribution, we will focus on prospects for tabletop coherent diffraction imaging by improving established sources and applying new sources. A major bottleneck of HHG powered CDI experiments, thus far, are the limited photon flux and the resulting long integration times. In the second section, we will present recent progress in employing ultrafast high-power fiber lasers for a high harmonic generation. Due to the high repetition rate, an unprecedented average power near the milliwatt level per harmonic order is achieved. Another promising source is a laser plasma-based tabletop soft X-ray laser (SXRL), which we will introduce in Sect. 35.3 as a light source for CDI experiments. The extraordinary high photon flux and the narrow line width make this source interesting for CDI. The potential of these sources is evaluated in the closing section.

35.2 High Photon Flux XUV and Soft X-Ray Sources Based on High Harmonic Generation with Femtosecond Fiber Lasers

High harmonic generation provides short wavelength radiation with very good beam quality and spatial coherence. However, the conversion efficiency is typically not larger than 10^{-6} into a single harmonic in the XUV and even lower for the soft X-ray spectral region [10].

Femtosecond fiber lasers have significantly advanced during the recent years and nowadays deliver up to millijoule pulse energies at repetition rates of up to 1 MHz [11]. The corresponding average output power can be as high as 1 kW, which is two orders of magnitude higher compared to typical Ti:Sapphire-based femtosecond lasers. Key issues for efficient HHG are pulse-shortening via post-compression [12] and a high-density gas target to achieve phase matching in the typically required tight-focusing regime [13].

The combination of such a high average power femtosecond fiber laser with hollow-fiber-based post-compression and subsequent HHG in a continuous high-density gas jet recently demonstrated more than 10^{13} photons/s (>100 μW average power) within a single plateau harmonic at 30 eV [14]. A similar HHG source has already successfully been used for sub-wavelength imaging at high numerical aperture [3]. In CDI experiments, a higher spatial resolution requires shorter wavelengths (higher photon energies) once a numerical aperture near unity is reached. For that reason, the operation range of the fiber laser-driven HHG source has been shifted to 70 eV. In the following subsections, work toward high photon flux at the aforementioned photon energy and extensions up to the soft X-ray regime will be presented.

35.2.1 High Photon Flux 70 eV HHG Source

Higher cutoff energies can be achieved in HHG by focusing the driving laser to higher intensities, using longer driving wavelengths, and using a target gas with higher ionization potential (argon in this case). Here, a 35 fs, 0.5 mJ laser is focused to a peak intensity of $>2 \cdot 10^{14}$ W/cm^2 onto an argon gas jet to generate XUV radiation up to ~70 eV. The photon flux at 68.6 eV (H57) was particularly optimized by tuning the gas pressure, the jet position, and an aperture in front of the focusing lens. A spatiotemporal profile of the detected harmonics is shown in Fig. 35.1. At 100 kHz repetition rate this XUV source reached $>10^{11}$ photons/s in this single 1.3 eV bandwidth harmonic [15]. Very recently, this source has been used for CDI experiments demonstrating a record sub-20 nm resolution enabled by the combination of short wavelength, high spatial coherence, and high photon flux [16].

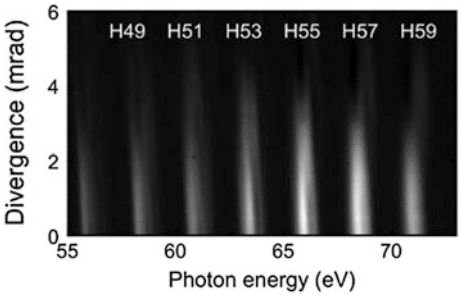

Fig. 35.1 Spatio-spectral distribution of high-order harmonics generated in argon

35.2.2 *High Photon Flux Coherent Soft X-Rays up to the Water Window*

HHG with a 1 μm wavelength laser into the soft X-ray region desires intensities on the order of 10^{15} W/cm^2 and very short (few-cycle) pulses to minimize the accumulated ionization of the target gas. These pulses can be generated efficiently by two-stage compression of a femtosecond fiber laser as described in [17]. Figure 35.2 displays typical HHG spectra that can be achieved with neon. Due to the few-cycle duration and a non-stabilized carrier-envelope phase, the harmonic lines are broadened and smeared out to a continuum. Nevertheless, a particular spectral region could be selected for imaging, e.g., by multilayer mirrors filtering a tailored central energy and bandwidth within the physical limits [18]. Although the conversion efficiency into the soft X-ray region is much lower compared to the XUV, still more than 10^9 photons/s/eV can be obtained up to the cutoff at ~150 eV (8 nm) [17].

HHG can be generated with this few-cycle laser in helium up to the so-called water window, but with a reduced photon flux due to poor phase-matching. Figure 35.2b displays measured spectra with and without an additional parylene filter clearly showing the carbon K-edge at 283 eV.

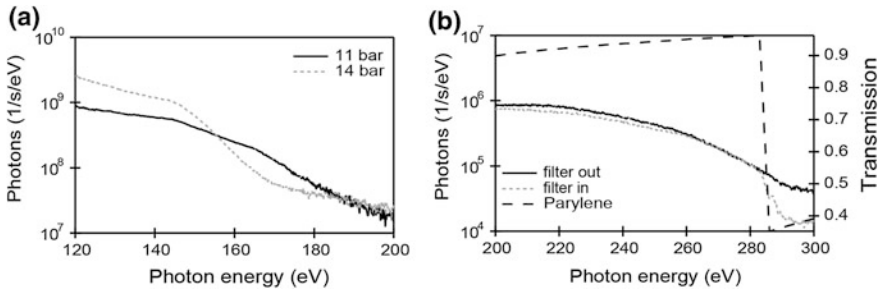

Fig. 35.2 **a** HHG spectra recorded with neon at different backing pressures of the gas jet. **b** HHG spectra ranging up to the water window with helium measured with and without an additional parylene filter

In the future, Tm-based fiber lasers delivering femtosecond pulses at 2 μm wavelength [19] will be employed to push the phase-matching cutoff into the water window and beyond. Thus, a new class of tabletop high photon flux soft X-ray sources will be available for tabletop imaging soon.

35.3 Solid-State Soft X-Ray Laser as Source for Coherent Diffraction Imaging

An alternative approach for generating coherent short wavelength radiation lies in employing plasma-based soft X-ray lasers (SXRL). These emit short pulses in the extreme ultraviolet XUV/soft X-ray range between 3 and 40 nm [20]. There are numerous schemes proposed for soft X-ray lasing, however, the transient collisional excitation scheme has proved to be the most reliable and promising for the development of compact laser-pumped SXRL [21]. It has been shown that combining this scheme with the grazing incidence (GRIP) pumping geometry a compact soft X-ray light source can be realized [22, 23]. Using about 1.5 J of pump energy in the GRIP scheme, strong XUV emission in the range between 10 and 20 nm with pulse energies of the SXRL up to 3 μJ were realized [24, 25]. Since the emission of the SXRL constitutes an atomic transition, the spectral bandwidth of the XUV emission is in the order of some picometer resulting in a very high temporal coherence [26]. Since these lasers typically operate in the self-amplified spontaneous emission (SASE) scheme, which is comparable to the operation scheme of most free-electron lasers, the transversal spatial coherence of the SXRL strongly depends on the geometry of the excitation scheme. The degree of spatial coherence ranges from few percents for a single-stage SXRL [27] up to 60% for a HHG-seeded X-ray laser [28]. For pump energies below 1 J, there are only very few data sets concerning the spatial coherence of a single stage laser. Nevertheless, these systems are worth further investigations, since they are attractive for applications requiring higher average photon flux, since pump lasers with pulse energies of 1 J or below are easily scalable to repetition rates up to 500 Hz [29].

Surprisingly, there are so far only very few examples of employing an SXRL for coherent diffraction imaging (CDI). For instance, in [30] an SXRL operating at 13.9 nm and pumped by a 1.5 J, 10 Hz Ti:Sa Laser was employed for coherent diffraction imaging. A spatial resolution of about 80 nm at 13.9 nm has been estimated at a numerical aperture of 0.08.

35.3.1 Molybdenum SXRL Operated with Moderate Pump Energy

Here, we report on recent experiments performed at an SXRL pumped in the GRIP geometry using moderate pump energies of below 0.5 J. The experimental layout is depicted in Fig. 35.3a. The soft X-ray laser was pumped by two pulses of a high repetition rate 100 Hz thin disk laser (TDL) chirped pulse amplification (CPA) system. The TDL system consists of a front-end with an Yb:KGW oscillator and stretcher delivering an output pulse of about 1 ns at 1030 nm. The stretcher is followed by a Yb:KGW regenerative amplifier. This output is subsequently divided into two pulses. Each of these pulses is amplified in a regenerative Yb:YAG thin disk amplifier to a level of about 100 mJ. The pulse from the first regenerative amplifier is compressed to a duration of about 200 ps using a grating compressor. The other pulse is fed to a thin disk multipass amplifier which amplifies the pulses to an energy up to 400 mJ. Subsequent compression in a grating compressor results in about 2 ps pulse duration. The long pulse (150 ps, $E \approx 70$ mJ) is focused by a combination of a cylindrical ($f = -500$ mm) and a spherical lens ($f = 380$ mm) onto the target at normal incidence. The resulting line focus has a width of about 30 μm. The generated plasma column is subsequently heated by the short pulse (2 ps, $E \approx 270$ mJ) focused according to the GRIP method by a spherical mirror ($f = 762$ mm) into the preformed plasma. In the presented case an optimal GRIP angle of 24° was found. The delay between the two pulses is a critical parameter [22, 23, 31], which can be set by the round trip time of the two amplifiers and a delay stage. Debris from the solid-state molybdenum target requires special attention at high repetition rate. In our experiments, we protected the optics against debris by thin glass plates or foils, and the SXRL output is guided through an aperture in order to reduce debris contamination on the following optical elements. The target itself is a Mo slab with a length of 50 mm and a width of 5 mm. An X-Y-Z scanning unit is synchronized with the laser and continuously moves the target such that a fresh spot is used every couple of laser shots. We found the most stable SXRL operation if the target surface was renewed after 5–10 laser shots. For a pulse combination of 70 mJ/150 ps in the long pulse and 270 mJ/2 ps in the short pulse, we estimated a lower limit for the energy of one single SXRL pulse of 100 nJ and a divergence of about 10 mrad. Typical beam profiles feature a rectangular-shaped mode being overlaid with higher frequency modulation. The latter is typical for SASE type lasers. The rectangular shape originates from the shape of the plasma column.

35.3.2 Coherent Diffraction Imaging Using the SXRL

In the CDI setup (Fig. 35.3a), the exit plane of the XUV source is imaged onto the sample with a demagnifying telescope consisting of two concave spherical mirrors

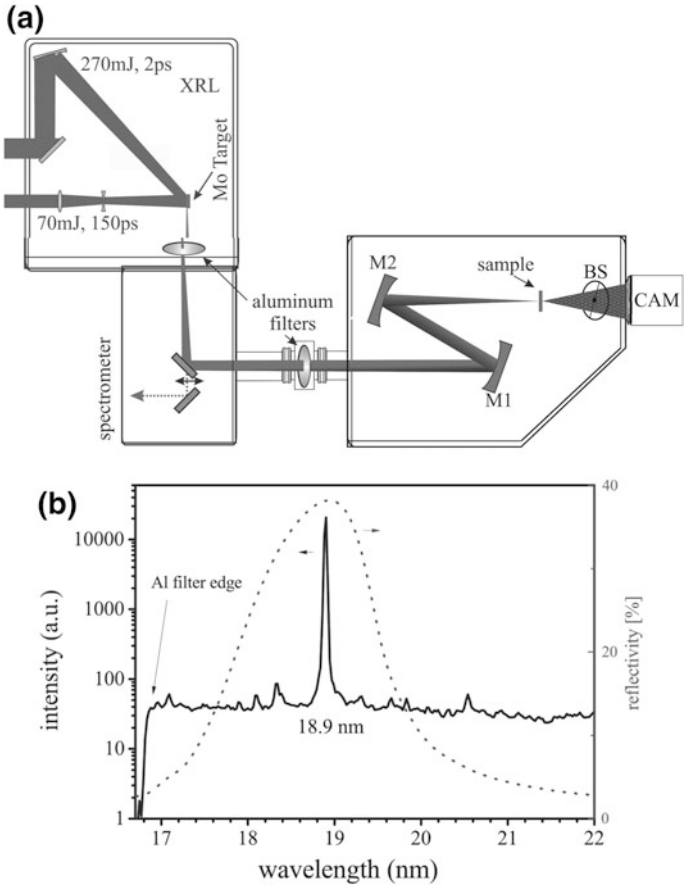

Fig. 35.3 **a** Typical experimental setup incorporating an SXRL and a CDI experiment. The molybdenum-based SXRL in this example emits at 18.9 nm (**b**). Aluminum filters suppress the stray light of the pump lasers and optically seal the experiment. Mirrors M1 and M2 are curved multilayer mirrors (**b**) that further spectrally clean up the SXRL beam and refocus the SXRL onto the sample. A back-illuminated cooled 16-bit CCD camera (CAM) measures the diffraction pattern

($ROC_1 = 2$ m, $ROC_2 = 1$ m) with a molybdenum/silicon multilayer coating. The mirrors are designed and optimized to have the highest reflectance coinciding with the SXRL emission line at 18.9 nm (Fig. 35.3b) [32]. Both multilayer mirrors have been realized with a dual ion beam deposition system described in [33]. From the model calculations and a reference measurement at the PTB synchrotron beamline at BESSY II a reflectivity of 14.6% (38.2% per single mirror, see Fig. 35.3b) under near normal incidence (2° off) at 18.9 nm was determined. In a CDI experiment a sample is placed in the rear focus of M2. The generated flux has been estimated prior to the imaging experiments with a calibrated XUV-sensitive photodiode. Under optimized conditions we obtained $(3.2 \pm 0.3) \times 10^{10}$ photons per shot,

which leads to an overall capability of the system of producing up to 3×10^{12} photons per second in less than 0.01% bandwidth centered around 18.9 nm.

In the presented experiment, we used a 50 nm thick silicon nitride membrane covered with a 50 nm thick gold layer on top. With a focused ion beam we milled a shaped aperture (see STEM image in inset in Fig. 35.4a) into this slab. The sample was introduced into the refocused XUV beam and the diffracted light was recorded with large area XUV/X-ray-sensitive CCD (Andor iKon L, 27.6×27.6 mm^2 chip size) positioned 15 mm downstream. The resulting numerical aperture is 0.67 allowing for a half-pitch resolution of 14 nm. Within 300 laser shots a typical diffraction pattern exhibiting fringes extending to the edge of the detector could be recorded (Fig. 35.4a). Even with a single laser shot diffraction patterns covering the inner 30% of the detector around the central speckle were measured.

For the iterative phase retrieval, we employed a guided version of the hybrid input–output algorithm that proved to work well in previous CDI experiments [3]. Unfortunately, the phase retrieval algorithm was neither able to reconstruct the full field of view nor very sharp edges (Fig. 35.4c). We attribute this to a limited spatial coherence. While the diffraction pattern features fringes that should at least support a spatial resolution around 20 nm, we get at best a resolution of about 400 nm, while it is difficult to assign a resolution if the object is not fully resolved. From the radially decaying signal in real space, we conclude that further distanced features of

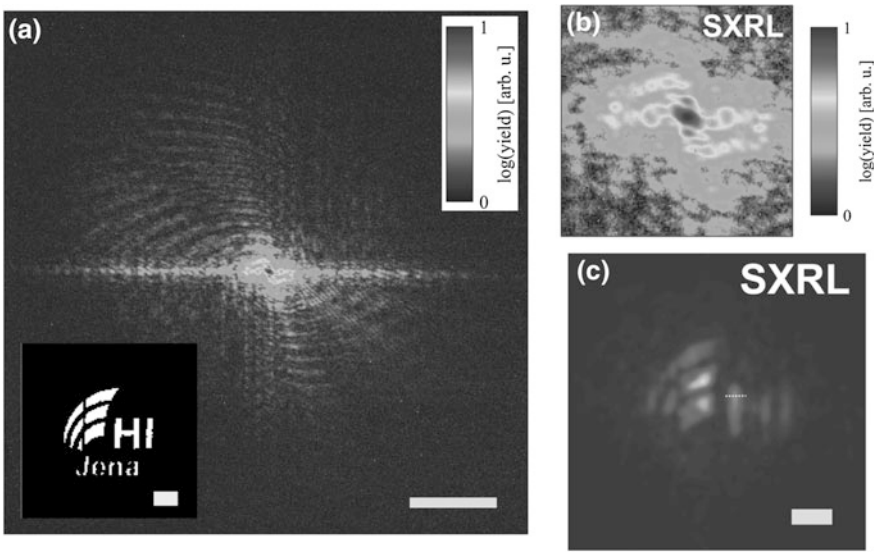

Fig. 35.4 Coherent diffraction imaging using a solid-state SXRL. **a** Measured diffraction pattern of an shaped aperture (STEM image inset) captured from 300 laser shots featuring fringes extending well to the edge of the detector. The scale bar in **a** is 10 μm^{-1} (inset 1 μm). **b** Detail of the diffraction pattern around zero momentum transfer. **c** The panel shows the modulus of the reconstructed real space (linear scale, scale bar 1 μm) for the SXRL measurement

the object produce speckles with reduced contrast which can consequently not be properly phased. The poor speckle contrast is also evident in Fig. 35.4b.

In this experiment we estimate the focal spot size to be roughly 15 μm full-width half maximum, while the object is 3 μm wide. A first analysis of the data suggests that for an object of about 1 μm width the spatial coherence would have been sufficient to phase out all speckles. The reconstruction quality should then be drastically improved since the decoherence observed in the presented experiment also compromises finding a proper support of the object which subsequently worsens the reconstruction. For smaller objects, however, the quality should be drastically improved.

Although the first measurements presented here resulted in low image quality due to the low spatial coherence, the speckles measured up to high momentum transfers in principle allowing sub-30 nm resolution within few laser shots justify more studies on these laser systems and more systematic investigations of the coherence properties [34].

35.4 Summary and Outlook

In this contribution, we have presented recent progress in the development of high-power ultrafast fiber lasers and discussed their capability of generating high harmonic radiation with high average power [35]. While the average power in the XUV approaches the milliwatt level, new developments allow scaling the photon energy into the energy range above 100 eV extending well into the water window. A combination of scaling toward higher photon energies and at the same time improving the flux should soon allow for coherent diffraction imaging at a spatial resolution at the 10 nm level. Short integration times will further allow for the application of these sources in tomographic and ptychographic scans in order to image three-dimensional and large volume specimen. To date, a spatial resolution down to 13 nm has been demonstrated using one of the presented fiber laser sources [16]. In contrast, SXRLs offer high pulse energies per shot confined in a very narrow linewidth making these lasers probably the best choice for single-shot imaging in a tabletop environment. The high average flux on the order of $>10^{12}$ photons/s in a picometer linewidth along with the scalability of the repetition rate of the presented thin disk pump laser hold promise for wide applicability in coherent diffraction imaging. One bottleneck experimentally observed is the limited spatial coherence of the SXRLs, which for now limits the usability to micron and sub-micron sized objects, e.g., bacteria, viruses, or particle clusters. Another possibility recently demonstrated to improve the flux and coherence property is a HHG-seeded SXRL [36] that essentially combines the best of two approaches.

Acknowledgements This work was partly supported by German Federal Ministry of Education and Research BMBF German–Korean collaboration program (01DR12011), the Korea–Germany program (Korean NRF 2010-00633, BK21), BMBF contracts 13N12082 “NEXUS” and 05P2015

"APPA," LaserLab Europe (INREX), EFRE (ProFit), the European Union's Seventh Framework Program (FP7/2007–2013)/ERC Grant agreement no [240460] "PECS," by the European Research Council under the ERC grant agreement no. [617173] "ACOPS" and the German Research Foundation (DFG) via the Excellence Cluster "Munich-Centre for Advanced Photonics" (MAP, EXC 158). M. Zürch acknowledges support from the Humboldt Foundation.

References

1. Sandberg, R.L., et al.: Studies of materials at the nanometer scale using coherent X-ray diffraction imaging. JOM **65**, 1208 (2013)
2. Krausz, F., Ivanov, M.: Attosecond physics. Rev. Mod. Phys. **81**, 163 (2009)
3. Zuerch, M., et al.: Real-time and sub-wavelength ultrafast coherent diffraction imaging in the extreme ultraviolet. Sci. Rep. **4**, 7356 (2014)
4. Zuerch, M., et al.: XUV coherent diffraction imaging in reflection geometry with low numerical aperture. Opt. Express **21**, 21131–21147 (2013)
5. Gardner, D.F., et al.: High numerical aperture reflection mode coherent diffraction microscopy using off-axis apertured illumination. Opt. Express **20**, 19050 (2012)
6. Shanblatt, E.R., et al.: Quantitative chemically-specific coherent diffractive imaging of reactions at buried interfaces with few-nanometer precision. Nano Lett. (2016). https://doi.org/10.1021/acs.nanolett.6b01864 (accepted manuscript)
7. Zuerch, M., et al.: Cancer cell classification with coherent diffraction imaging using an extreme ultraviolet radiation source. J. Med. Imaging **1**, 031008 (2014)
8. Witte, S., et al.: Lensless diffractive imaging with ultra-broadband table-top sources: from infrared to extreme-ultraviolet wavelengths. Light Sci. Appl. **3**, e163 (2014)
9. Thibault, P., et al.: High-resolution scanning X-ray diffraction microscopy. Science **321**, 379–382 (2008)
10. Winterfeldt, C., et al.: Colloquium: optimal control of high-harmonic generation. Rev. Mod. Phys. **80**, 117–140 (2008)
11. Müller, M., et al.: 1 kW 1 mJ eight-channel ultrafast fiber laser. Opt. Lett. **41**, 3439–3442 (2016)
12. Hädrich, S., et al.: 200 W average power energetic few-cycle fiber laser. In: High-Brightness Sources and Light-Driven Interactions, p. JT3A.1. Optical Society of America (2016)
13. Rothhardt, J., et al.: Absorption-limited and phase-matched high harmonic generation in the tight focusing regime. New J. Phys. **16**, 033022 (2014)
14. Hädrich, S., et al.: High photon flux table-top coherent extreme ultraviolet source. Nat. Photonics **8**, 779–783 (2014)
15. Rothhardt, J., et al.: High-repetition-rate and high-photon-flux 70 eV high-harmonic source for coincidence ion imaging of gas-phase molecules. Opt. Lett. **24**(16), 18133–18147 (2016)
16. Tadesse, G.K., et al.: High speed and high resolution table-top nanoscale imaging. Opt. Lett. **41**(22), 5170–5173 (2016)
17. Rothhardt, J., et al.: 53 W average power few-cycle fiber laser system generating soft X rays up to the water window. Opt. Lett. **39**, 5224 (2014)
18. Guggenmos, A., et al.: Chromium/scandium multilayer mirrors for isolated attosecond pulses at 145 eV. Opt. Lett. **40**, 2846–2849 (2015)
19. Stutzki, F., et al.: 152 W average power Tm-doped fiber CPA system. Opt. Lett. **39**, 4671–4674 (2014)
20. Suckewer, S., Jaegle, P.: X-ray laser: past, present, and future. Laser Phys. Lett. **6**, 411–436 (2009)
21. Nickles, P.V., et al.: Short pulse X-ray laser at 32.6 nm based on transient gain in neon-like titanium. Phys. Rev. Lett. **78**, 2748–2751 (1997)

22. Tuemmler, J., et al.: 10-Hz grazing incidence pumped Ni-like Mo X-ray laser. Phys. Rev. E **72**, 0374011–0374014 (2005)
23. Keenan, R., et al.: High-repetition-rate grazing-incidence pumped X-ray laser operating at 18.9 nm. Phys. Rev. Lett. **94**, 1039011–1039014 (2005)
24. Wang, Y., et al.: Demonstration of high-repetition-rate tabletop soft-X-ray lasers with saturated output at wavelengths down to 13.9 nm and gain down to 10.9 nm. Phys. Rev. A **72**, 7 (2005)
25. Cassou, K., et al.: Optimization toward a high-average-brightness soft-X-ray laser pumped at grazing incidence. Opt. Lett. **32**, 139–141 (2007)
26. Hasegawa, N., et al.: High-precision measurement of the spectral width of the nickel-like molybdenum X-ray laser. JCPS **163**, 012062 (2009)
27. Lucianetti, A., et al.: Transverse spatial coherence of a transient nickellike silver soft-X-ray laser pumped by a single picosecond laser pulse. Opt. Lett. **29**, 881–883 (2004)
28. Wang, Y., et al.: High-brightness injection-seeded soft-X-ray-laser amplifier using a solid target. Phys. Rev. Lett. **97**, 123901/1-4 (2006)
29. Baumgarten, C., et al.: 1 J, 0.5 kHz repetition rate picosecond laser. Opt. Lett. **41**, 3339–3342 (2016)
30. Kang, H.C., et al.: Single-pulse coherent diffraction imaging using soft X-ray laser. Opt. Lett. **37**, 1688–1690 (2012)
31. Luther, B.M., et al.: Saturated high-repetition-rate 18.9-nm tabletop laser in nickellike molybdenum. Opt. Lett. **30**, 165–167 (2004)
32. Guggenmos, A., et al.: Ion polished Cr/Sc attosecond multilayer mirrors for high water window reflectivity. Opt. Exp. **22**, 26526–26536 (2014)
33. Guggenmos, A., et al.: Aperiodic CrSc multilayer mirrors for attosecond water window pulses. Opt. Express **21**, 21728–21740 (2013)
34. Zürch, M., et al.: Transverse coherence limited coherent diffraction imaging using a molybdenum soft X-ray laser pumped at moderate pump energies. Sci. Rep. **7**, 5314 (2017)
35. Klas, R., et al.: Table-top milliwatt-class extreme ultraviolet high harmonic light source. Optica **3**(11), 1167–1170 (2016)
36. Depresseux, A., et al.: Table-top femtosecond soft X-ray laser by collisional ionization gating. Nat. Photonics **9**, 817–821 (2015)